Grasp planning for thin-walled deformable objects

Nicolas Alt, Jingyi Xu and Eckehard Steinbach

Chair of Media Technology, Technische Universität München, 80333 München, Germany

Email: {n.alt, jingyi.xu, eckehard.steinbach}@tum.de

Abstract—**In this work, we consider the challenge of grasping thin-walled deformable objects like plastic bottles and other containers, which are very common in household environments. The deformability of such objects varies considerably along their surface, depending on the local geometry. To consider such phenomenon, we propose a grasp planner, which first uses the Finite Element Method (FEM) for deformation simulation to pre-calculate the map of local stiffness and then determines feasible grasp points based on this map. Experiments with a two-finger gripper are performed in order to verify the predicted grasp points.**

Index Terms—**Grasping, Deformable models.**

Introduction: Deformable objects change their shape when a force is applied to them during a manipulation process. This behavior must be considered for the planning of manipulation tasks, such as grasping. Thus, we present an grasping approach, which is especially suited for objects with deformation characteristics that are strongly correlated with their geometry, such as plastic bottles, cups or other containers. The stiffness of objects is represented by a so-called stiffness map, which is obtained from a geometric object model by elasticity simulation with the Finite Elements Method (FEM). This process may be performed offline for a large object database. Next, a grasp score is calculated, which considers the magnitude of deformation based on the stiffness map, as well as local geometry features. We limit our discussion to grasps with two contact points in this paper and briefly discuss extensions to multi contact grasps in the conclusion.

Related work: Previously, robot manipulation mainly focused on rigid objects. GraspIt [1] is a generic grasping simulator for various robotic hands. The simulator is able to analyze the quality of a grasp in real-time. Deformable objects, however, are not considered. More recently, several manipulation approaches for deformable objects have been presented. In [2], a method is presented for manipulating deformable food and learn its haptic properties. An approximation of deformation costs of pillows and cloths with Gaussian regression is proposed in [3]. A drawback of these approaches is that they are limited to deformable objects with roughly uniform stiffness. In [4], a method is proposed to estimate internal states of thin-walled objects, which used tactile features and real objects as training set.

Local stiffness: Thin-walled objects show great variations in deformability (or hardness) on their surface, depending on how forces are diverted. Large, flat surface areas are typically soft, while convex areas or areas with nearby support structures are rather hard. The deformation behavior of a single point is referred to local stiffness, i.e. its force-deformation curve, which is represented by a low order model. In a linear model, the coefficient has the unit $\frac{N}{m}$, which corresponds to the spring stiffness in Hooke's law. The stiffness component perpendicular to the surface varies most and is also most relevant for grasping. Thus, only this single component of stiffness is considered. To represent the linear stiffness coefficient perpendicular to the surface, we calculate the so-called stiffness maps in a simulation process. For large databases of geometric object models, it is feasible to pre-calculate the stiffness maps.

Simulation of elasticity is performed with the Finite Element Method (FEM) on synthetic object models. Alternatively, the models

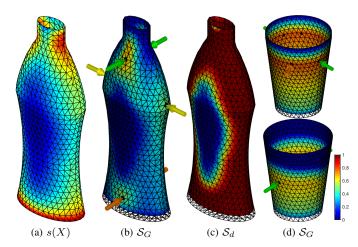(a) $s(X)$ (b) $\mathcal{S}_G$ (c) $\mathcal{S}_d$ (d) $\mathcal{S}_G$

Fig. 1: Stiffness map (a), grasping scores (b) and deformation score (c) for a plastic bottle. (d) shows the grasp score for a plastic cup with/without reinforcement ring. The detected grasp patterns are indicated by arrows in (b) and (d).

can be generated by multi-view reconstruction with a depth camera. In many cases, only surface models are available. An extension to volumetric models of thin-walled objects is straight-forward by adding a second wall towards the inside of the existing surface. Besides geometry information, volumetric elements also contain material parameters, such as the elastic modulus E and the Poisson's ratio ν. Material parameters and wall thickness must be given manually.

Besides an object model, FEM simulation requires boundary conditions, which are given as forces or displacements for any node. We used Vega FEM library [5] for the simulation. For each set of boundary conditions, a deformed shape, i.e. the displacement of all nodes is obtained. Here, we are only interested in the static solution, since dynamic effects can be neglected for typical manipulation velocities used by robots in unstructured environments. Boundary conditions consist of an object fixture on the ground, and the representation of a varying grasp pattern. The simplest realistic grasp pattern that provides is represented by two single contact points on opposing sides of the object. The forces of the two points are perpendicular to the contact surfaces and directed in opposing directions, thus result in a zero global force. The grasp pattern corresponds to two point stimuli applied as a force boundary condition to two opposing nodes on the outer surface of the object. Examples for these grasp patterns are indicated by arrows in Fig. 1b. The simulation is repeated for all points on the outer surface with a constant grasping force F_G for linear models or multiple forces for higher order models. The linear stiffness coefficient $s(\boldsymbol{x})$ of point $\boldsymbol{x} = [x, y, z]$ is obtained from the resulting displacement at this point:

$$s(\boldsymbol{x}) = \left. \frac{F_G}{|d(\boldsymbol{x})|} \right|_{\text{Grasp at } \boldsymbol{x}}$$

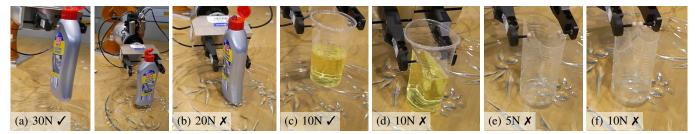(a) 30N ✓ (b) 20N ✗ (c) 10N ✓ (d) 10N ✗ (e) 5N ✗ (f) 10N ✗

Fig. 2: Grasping experiments with real objects confirm the predicted grasp plans, see Fig. 1.

Only the local deformation at the touch point is considered in $s(\boldsymbol{x})$, i.e. any shape change beyond the touch point is ignored.

Grasping score: The goal of grasp planning is to find "stable" grasp configurations for a given object and gripper. This means that the object pose is determinate and remains fixed with respect to the gripper during the grasping process. Grasp forces must be chosen large enough to avoid slipping or tilting of the object, which requires the consideration of surface friction, weight and center of mass of the object. We propose a grasp score for deformable objects based on local stiffness maps. The deformation resulting from a given grasping force must remain within an acceptable range, i.e. the shape change caused by the grasp must not be too large. Furthermore, this avoids destruction of the object or spilling of the liquid inside the container. Candidates of grasp patterns used in simulation are dual point contacts on opposing points of the object. The feasibility of each pattern is determined by a score $\mathcal{S}_G$, which consists of four components introduced below. Each component is associated with a weight value $w_\star$. These simple features are only used to present feasible grasp configurations. More sophisticated approaches exist in related work, such as [1].

a) Deformation: As discussed, deformation must remain below a threshold δ_{max} for a given grasping force. Both values must be given manually or by considering additional model parameters.

$$\mathcal{S}_d(\boldsymbol{x}) = -\frac{1}{2} \tanh \left[w_d \left(s^{-1}(\boldsymbol{x}) \cdot F_G \cdot \delta_{max}^{-1} - 1 \right) \right] + \frac{1}{2}$$

The score is 1 for small deformations, and 0 for large ones, see Fig. 1c. A soft transition is ensured by the $\tanh$ function, whereby the transition width is adjusted by w_d.

b) Contact: The object surface normal $\mathbf{n}(\boldsymbol{x})$ and the direction of the applied force should be preferably parallel to avoid slip. The contact score considers a neighborhood $\mathcal{N}$ of points within d around the current surface point $\boldsymbol{x}$:

$$\mathcal{S}_n(\boldsymbol{x}) = \frac{w_n}{||\mathcal{N}_d(\boldsymbol{x})||} \sum_{\xi \in \mathcal{N}_d(\boldsymbol{x})} \left(1 - \sqrt{||\xi - \boldsymbol{x}|| d^{-1}} \right) \mathbf{F} \cdot \mathbf{n}(\xi)$$

Furthermore, a merely partial overlap between the finger and the object is penalized.

c) Curvature: Similarly, grasp points within locally flat or concave surface areas avoid slipping on the surface. Points $\mathcal{N}_d(\boldsymbol{x})$ are rotated by aligning the $\mathbf{n}(\boldsymbol{x})$ with the z-axis, and a second-order polynomial surface is fitted to them. The curvature score $\mathcal{S}_C$ is calculated from the quadratic coefficients of this surface, according to: $\mathcal{S}_c = 1 + w_c \min \{p_{20}, p_{02}\}$.

d) Height bias: Objects grasped by two contact points are susceptible to tilting if grasped below their center of mass. A height bias favours grasp points that lie closer to the top of the object: $\mathcal{S}_h(\boldsymbol{x}) = (1 - w_h) + w_h \frac{z}{\max(z)}$.

The final grasp score $\mathcal{S}_G$ is calculated online from the stiffness map by cutting all components to the range $[0; 1]$ and multiplying them, see Fig. 1b and Fig. 1d. The coefficients are chosen according

to the physical properties of the gripper, such as contact area and lateral stability. Here, we use $w_d = 5.0, w_n = 1.0, w_c = 5.0, w_h = 0.5, \delta_{max} = 5\text{mm}$ and $d = 1\text{cm}$. Generally, there are multiple feasible grasp configurations (e.g. $\mathcal{S}_G > 0.5$). The optimal configuration also considers costs from an arm trajectory planner.

Experiments: A grasping experiment (Fig. 2), is conducted for three different objects: the bottle of a cleaning agent (Fig. 2a), a thin plastic cup with an reinforcement ring on top (Fig. 2c) and the same cup without this ring (Fig. 2e). Grasp scores and plans from the proposed estimator are shown for these models in Fig. 1. The two predicted grasp configurations for the (open) cleaner, near the lid and on the side, work successfully (Fig. 2a). The grasp on the side, however, is very sensitive to alignment errors, which is expressed by a low curvature score $\mathcal{S}_c$. A grasp with 20N at the center of the object (Fig. 2b), however, results in spilling of liquid contents. The predicted grasp on the top of the cup with an reinforcement ring also succeeds (Fig. 2c). Fig. 2d illustrates that a grasp with the same force in the center results in a large, permanent deformation of the cup. Without the reinforcement ring on the top (Fig. 2e, Fig. 2f), a force of 5N and 10N results in a large deformation, and the object slips out of the gripper, even if it is empty. The two-finger gripper with two tips used in the experiments corresponds to an ideal dual contact grasp pattern as used in the simulation. Other finger designs, such as fingers with a soft laminar material, might be better-suited for the presented objects. Yet, note that each mechanical design has its own strength and limitations, which must be considered accordingly by parameters in the planning process.

Conclusion and outlook: We present a grasp planner for thin-walled objects, such as bottles, which selects grasp points based on the local stiffness of the object surface. Stiffness maps are obtained by an FEM-based simulation of elasticity, applying generic grasp patterns to the object. In future work, the proposed deformability score will be integrated into existing grasp planners, such as GraspIt [1]. Multiple grasp points will be considered by a coupling matrix, which represents the mutual influence of grasp points. Finally, methods for the automatic calculation or learning of the various parameters will be presented.

REFERENCES

[1] A. T. Miller and P. K. Allen, "Graspit! a versatile simulator for robotic grasping," *Robotics & Automation Magazine, IEEE*, vol. 11, no. 4, 2004.

[2] M. C. Gemici and A. Saxena, "Learning haptic representation for manipulating deformable food objects," in *Int. Conf. on Intelligent Robots and Systems (IROS)*. IEEE, 2014.

[3] B. Frank, C. Stachniss, N. Abdo, and W. Burgard, "Efficient motion planning for manipulation robots in environments with deformable objects," in *Int. Conf. on Intelligent Robots and Systems (IROS)*. IEEE, 2011.

[4] S. Chitta, J. Sturm, M. Piccoli, and W. Burgard, "Tactile sensing for mobile manipulation," *Robotics, IEEE Transactions on*, vol. 27, no. 3, pp. 558–568, 2011.

[5] F. S. Sin, D. Schroeder, and J. Barbič, "Vega: Non-linear fem deformable object simulator," *Computer Graphics Forum*, vol. 32, no. 1, 2013.